GCAGS JOURNAL
A Publication of the Gulf Coast Association of Geological Societies
www.gcags.org

Back-Reef Depositional Environments in a Lower Cretaceous (Sligo) Shelf-Margin Complex: Insights into Ultradeep Reservoir Preservation and Controls on Stacking Patterns in an Outer Platform Setting

Kelly E. Hattori, Robert G. Loucks, and Hongliu Zeng

Bureau of Economic Geology, The University of Texas at Austin, P.O. Box X, Austin, Texas 78713, U.S.A.

ABSTRACT

The Early Cretaceous Sligo and Stuart City shelf-margin trends in Texas have been a subject of interest for over 60 years, attracting attention both because of their striking complex reef lithologies and their continued potential for oil and gas exploration. Numerous gas reservoirs have been discovered since the late 1950s, with a major push for revitalization and expansion occurring in the 2000s. The shelf-margin complexes originated as steep-walled reefs rimming the Comanche Platform. They evolved into a narrow (<6 mi) highly heterogeneous belt of banks, islands, shoals, and tidal flats with an associated highly productive shallow-water carbonate factory. Most characterization efforts for these systems have focused on known reservoirs in South Texas; very little work has investigated the margins outside of this region, particularly with respect to the Sligo shelf margin. This investigation presents the first well-documented long stratigraphic section for the Sligo margin in East Texas, which serves as an initial step in understanding this major shelf-margin complex. Facies are mainly associated with back-reef to back-reef lagoon environments and exhibit significant heterogeneity on the basis of variations in water depth and wave energy, with facies including argillaceous carbonate mudstones, oncolitic packstones, rudist biostromes, reef-derived grainstones, ooid grainstones, and algal laminate bindstones. Four depositional sequences are delineated based on broad changes in facies and stacking patterns related to water depth and energy regime, yielding new insight into controls on facies partitioning in a stable long-term shelf-margin complex. The pore network, which is limited to micropores, is largely facies-controlled and is related to the presence of originally Mg–calcite allochems such as miliolids and *Lithocodium/Bacinella*. As East Texas has significant structural complexity, the ultradeep buried Sligo Formation is an underexplored area with the potential for undiscovered reservoirs related to structural features. Geologic characterization of this core is an important step in understanding some of the porous lithofacies present within the Sligo shelf margin in East Texas.

INTRODUCTION

The Lower Cretaceous Sligo and Stuart City (Edwards) shelf margins have been a target for potential gas production in Texas since the initial discovery in the 1950s (Cook, 1979). Several fields, including the highly productive Pawnee and Word fields, were discovered early, with new discoveries and successes tapering off after the 1970s. Revitalization of this play in the early 2000s by Pioneer Natural Resources Co. saw several new significant gas discoveries and much-improved production from existing fields, which was achieved by a massive upscaling in data acquisition (deep pilot holes with full wireline-log suites, long cores, and extensive 2D and 3D seismic surveys) that vastly improved understanding of the shelf-margin system (Waite, 2009).

A challenge in exploring these deeply-buried margins is the amount of risk and unknowns. After a robust characterization campaign, Waite (2009) demonstrated that the Lower Cretaceous shelf margins had significant heterogeneity in almost every aspect, from facies to stratal architecture to reservoir properties. Several studies have endeavored to characterize different aspects of these margins, including facies and depositional settings (Bebout and Loucks, 1974; Achauer, 1977; Bebout, 1977; Bebout et al., 1977, 1981; Kirkland et al., 1987; Scott, 1990; Phelps et al., 2014), stratal architectures (Bay, 1977; Wooten and Dunaway, 1977; Kirkland et al., 1987; Winker and Buffler, 1988; Fritz et al., 2000), diagenesis (Bebout et al., 1977, 1981; Perkins, 1989; Loucks et al., 2013), and specific reservoir-scale characterization (Waite, 2009; Loucks et al., 2013; Van Simaeys et al., 2017). However, most studies focus primarily on the Stuart City trend, with the Sligo margin remaining understudied partly be-

Manuscript received May 24, 2023; revised manuscript received August 17, 2023; manuscript accepted August 17, 2023.

GCAGS Journal, v. 12 (2023), p. 17–32.
https://doi.org/10.62371/HGLG8668

cause of its deep burial and corresponding lack of deep wells and cores to examine.

Nevertheless, the Sligo trend remains an area of interest. Dry gas production has been established in several fields, including Pawnee and Kenedy SW, but otherwise, development has been slow. This may be attributable to the margin's ultradeep burial or the presence of sulfuric acid, both of which increase drilling costs. Furthermore, the Sligo shelf-margin complex may need more rigorous, higher-resolution characterization: Waite (2009) conclusively demonstrated considerable variability in the overlying Stuart City trend, which significantly improved subsequent exploration efforts. Further characterization studies of the deeper, earlier Sligo margin, as conducted by Pioneer (Waite, 2009) for the later Stuart City margin, may potentially yield similar results.

The primary goal of this study is the detailed characterization of the long cored interval of the Humble No. 1 Howell well in Tyler County, with the intent of establishing it as the type section for the Sligo margin back-reef setting in East Texas. Specific goals are to (1) define the facies and associated conditions and processes that formed them; (2) group the facies into depositional environments; (3) establish stacking patterns; (4) review the paragenetic history of these deeply buried limestones; and (5) analyze pore networks that contribute to ultradeep carbonate reservoirs in shelf-margin complexes. The study of facies, depositional environments, diagenesis, and control on potential reservoirs will provide useful concepts for exploration and development in the East Texas portion of the Sligo margin-reef trend.

GEOLOGIC SETTING

Throughout the majority of the Early Cretaceous, the northern rim of the Gulf of Mexico was a site of major tropical carbonate accumulation, with the widespread Comanche Platform first initiating as a distally-steepened ramp and maturing into a rimmed platform (McFarlan and Menes, 1991; Goldhammer and Johnson, 2001; Phelps et al., 2014; Loucks et al., 2017). Five intervals of reef accretion at the shelf margin mediated this change in architecture: the Knowles (Berriasian), Calvin (Valanginian), Winn (Valanginian), Sligo (Hauterivian-Aptian), and Stuart City (Edwards) margin (Albian) (Fig. 1). Of the five, the Sligo and Stuart City margins have garnered the most interest, being robust with strongly developed long-lived reef tracts and significant associated petroleum potential. The aggradational to progradational steep-walled reef rims continuously grew upwards towards sea level, trapping sediment and facilitating the development of a vast platform interior consisting mainly of shallow-water environments with some deeper intrashelf basins (Fig. 2).

In addition to affecting sediment deposited in the platform interior, the reefs significantly impacted local facies architecture at the shelf margin. As reefs grow toward sea level, they modify local water depth, wave and current energy, and sedimentation patterns (Immenhauser, 2009; Schlager, 2010; Purkis et al., 2015). During periods of long-lived reef accretion and expansion, the margin may transform into a complex shallow-water carbonate factory, with islands, banks, shoals, and peritidal settings developing along the raised outer shelf margin bordered on the seaward side by the basin and on the landward side by a deeper shelf lagoon (Schlager, 1981, 2003). Although relatively narrow (<6 mi wide), these shelf-margin complexes are highly heterogeneous with respect to stratal architectures and facies distributions, making their characterization difficult in the subsurface where data density is a challenge. Thus, rigorous investigation and integration of seismic to core-scale data is needed to infer facies relationships and depositional settings.

The Sligo and Stuart City margins are both characterized by similar fauna and depositional settings, although facies architectures and distributions vary. Some studies have identified a large suite of facies associated with the Sligo shelf-margin complex,

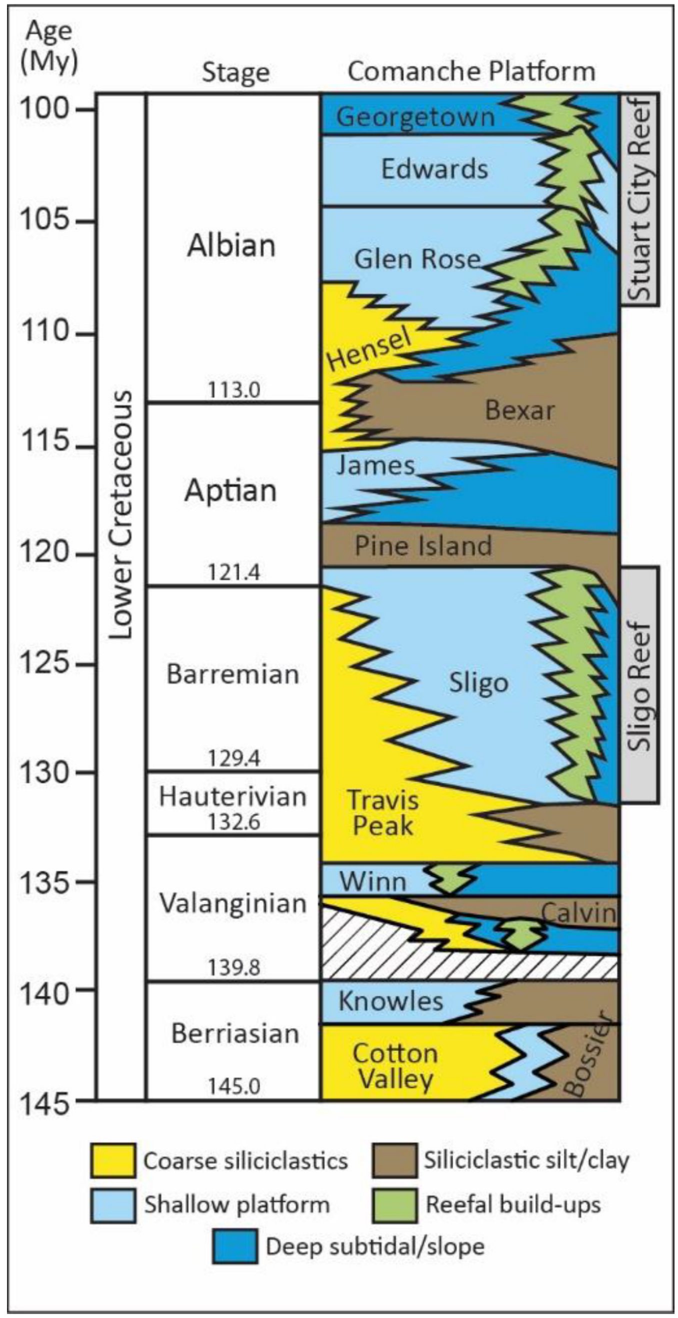

Figure 1. Regional stratigraphic column for the upper Lower Cretaceous Comanche Platform with generalized depositional profiles and lithologies (modified after Phelps et al. [2014] and Loucks et al. [(2017] and updated with most recent stage boundary ages from the International Commission on Stratigraphy [Cohen et al., 2013, 2023]).

particularly in the wider back-reef setting: Achauer (1977) reviewed five cores in Bee, Dewitt, Duval, Karnes, and Waller Counties; Bebout (1977) and Bebout et al. (1981) characterized several cores in South Texas spanning Bee, Dewitt, Duval, Karnes, La Salle, and Webb counties; and Phelps et al. (2014) characterized two cores in Karnes and Bee counties. The earlier work by Achauer (1977) recognized a reef proper consisting of corals, rudists, hydrozoans, and algal boundstones and skeletal debris grainstones; just landward, he documented a back-reef environment consisting of miliolid-peloid skeletal wackestone and grainstone interbedded with subordinate units of reef-derived

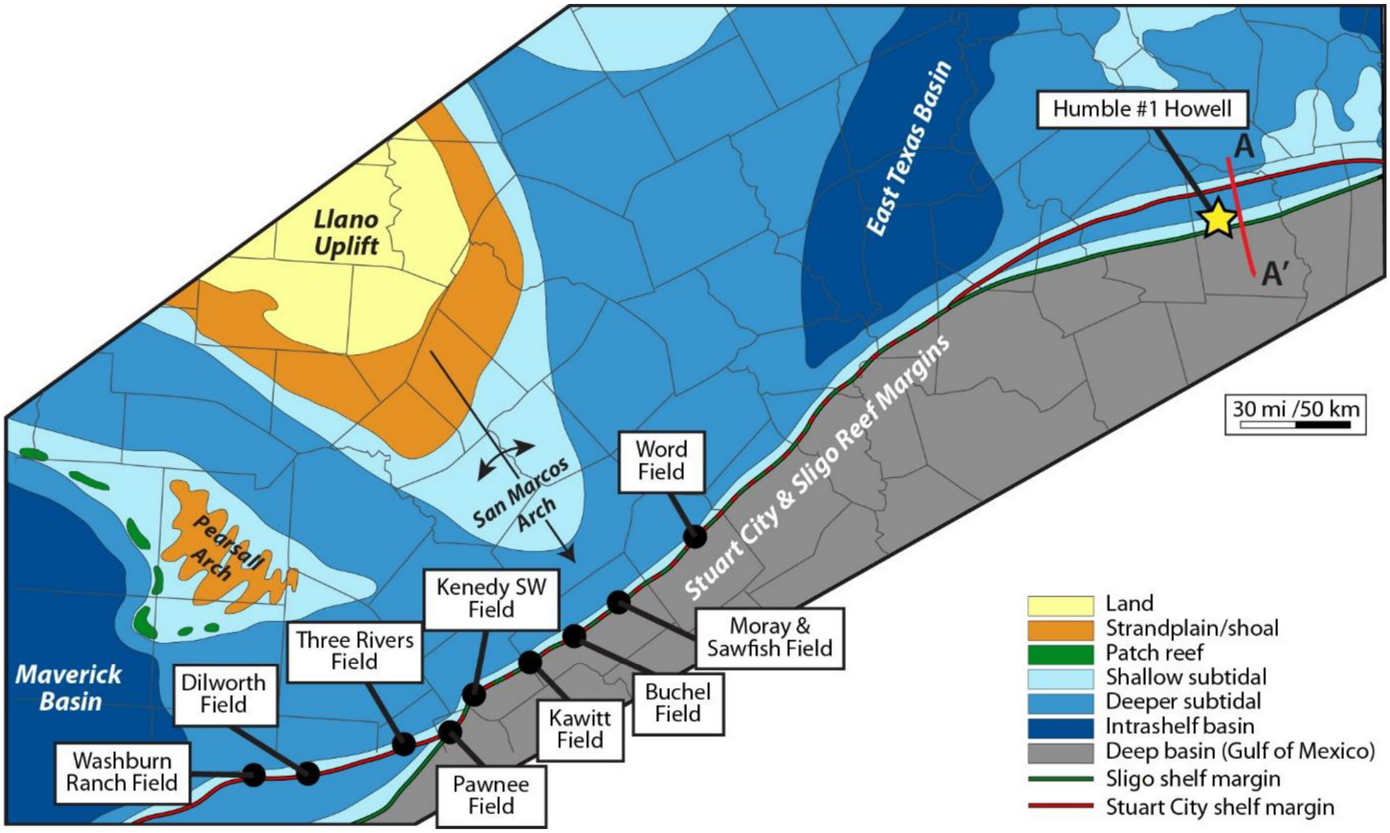

Figure 2. Paleogeography of the Comanche Platform, depicting both Sligo and Stuart City shelf margins and their relationships to each other. Productive shelf-margin trend fields in South Texas are labeled, as well as the location of the Humble No. 1 Howell well. The red line denotes the location of seismic line A–A'.

grainstone, packstone, and wackestone. Further work published by Bebout (1977) and Bebout et al. (1981) added additional detail to the back-reef facies model, identifying a suite of seven facies that can be attributed to a lower-energy back-reef setting: fossiliferous lime mudstone, oyster-miliolid wackestone, toucasid wackestone, oncolite packstone, laminated lime mudstone, coated-grain packstone, and pellet (peloid) packstone. They, too, recognized similar reef and shoal facies as Achauer (1977) as part of the shelf-margin bank and shoal complex. Phelps et al. (2014), in their presentation of a broader-scope detailed sequence stratigraphic assessment of the subsurface Lower Cretaceous in South Texas, largely agreed with the characterization of Bebout et al. (1981) and placed the shelf-margin successions within their stratigraphic framework for the Comanche Platform, contextualizing observed larger-scale stacking patterns in the scope of eustatic fluctuations.

Few studies have addressed internal heterogeneity within the reef trends at a higher-resolution scale. Intensive characterization efforts by Waite (2009) revealed that the Stuart City margin in South Texas can be divided into two distinct periods of reef growth. The upper Stuart City is composed of transient rudist-dominated fauna distributed in a system similar to a modern Bahamian reef-shoal environment. In contrast, the lower Stuart City is dominated by more organized reef frameworks, such as rudist-coral-stromatoporoid boundstones, in a system reminiscent of modern barrier reefs in Belize. These two Stuart City systems are shown to have distinctly different architectures and associated facies mosaics, highlighting the need for increasing characterization efforts elsewhere to improve understanding of the Lower Cretaceous shelf-margin trends at an informative and practical resolution.

East Texas has been heavily impacted by basement structural features, faulting, uplift, and salt tectonics throughout its history (Jackson and Seni, 1983; Ewing, 1991, 2009; Adams, 2009). These features drove the development of a complex and ever-changing topography, which could have impacted reef development and shelf-margin complex architecture during deposition, reservoir development, and hydrocarbon migration and trapping. As such, the East Texas region continues to present additional challenges and opportunities.

DATA AND METHODS

The study focuses on a core from the Humble No. 1 Howell well in Tyler County, Texas. Several long cores were obtained from the well, two of which recovered sections of the lower Sligo interval totaling 373 ft thick (Fig. 3). The lower core in the Sligo recovers an interval from 17,928 ft to 18,198 ft; after a 43 ft gap, the upper core in the Sligo recovers an interval from 17,885 to 17,825 ft. Routine core analysis was performed on these cores, including core description, facies delineation, sampling for thin sections, and scanning electron microscopy (SEM) analysis. No x–ray diffraction (XRD) or core-plug porosity or permeability analyses were conducted. Facies types were assigned to interpreted depositional environments, and stacking patterns were used for sequence stratigraphic interpretation.

Petrographic analysis was conducted on 45 thin sections collected from representative sections of all facies described in the core. For each thin section, mineralogy, texture, allochem type and abundance, diagenetic features, and pore types and distribution were assessed. Thin sections were impregnated with

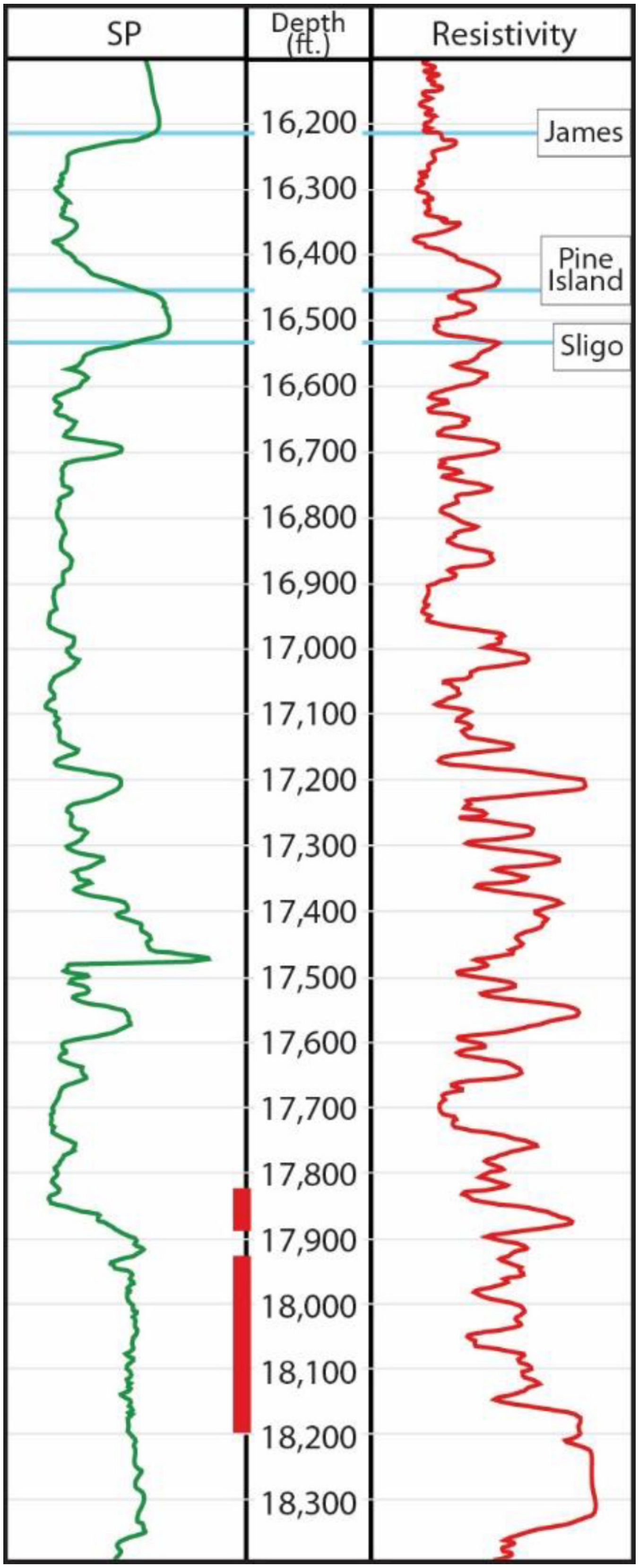

Figure 3. Wireline log for the Humble No. 1 Howell well. James, Pine Island, and Sligo formation tops are delineated by light blue lines and labeled. Cored intervals studied are shown by vertical red bars.

blue epoxy to emphasize macropores and with blue fluorescent dye to highlight macropores under fluorescent light.

The dip seismic section A–A' (courtesy of Fairfield Geotechnologies, previously ION GulfSpan line GSM3–2150) shows regional structure and stratigraphic framework and provides useful calibration to the interpretation of stratigraphy and facies of this core (Fig. 4). In particular, it provides critical insight into the placement of the No. 1 Howell well relative to the Sligo shelf margin, as well as demonstrating the relationship between the outboard Sligo shelf margin and the backstepped overlying Stuart City shelf margin. A well-to-seismic correlation was established using synthetic seismograms at the No. 1 Howell well (Fig. 5). The major character tie between synthetics and well-site seismic traces appears clear. Major seismic stratigraphic reference horizons are the synthetic trace's relatively strong-amplitude events (i.e., peaks and troughs) and are traceable throughout the seismic line (e.g., top Cretaceous, Austin Chalk, Pearsall, and Sligo). They were then used to define major stratigraphic sequences and platform-margin architecture in the study area. One issue of concern is that the No. 1 Howell well is located approximately 12 mi west of the seismic line A–A'. As a result, the synthetic tie is not exact, and a certain error may exist. Considering that the early Cretaceous margin in the Gulf of Mexico (especially the Sligo margin, Fig. 2) was very stable without significant migration in strike direction, a perpendicular projection of the well to seismic line still seems a correct representation of the geologic model for the seismic response. Based on this well-seismic correlation, the Stuart City margin and Sligo margin can be clearly defined on the flattened seismic section (Fig. 4). The relationship between the well and those margins becomes simple to interpret. General seismic facies are recognized around the well (e.g., mound facies in front of cored section and back of mound facies at the cored section) that can assist in the interpretation of the geological setting of the core.

LITHOFACIES

Eleven lithofacies were delineated to describe changes in rock fabric, allochem type/abundance, and depositional setting. These facies are organized into four facies associations based on general interpreted depositional settings: (1) peritidal; (2) high-energy shallow subtidal; (3) low- to moderate-energy shallow subtidal; and (4) low-energy deep subtidal.

Facies Association 1: Peritidal

The peritidal facies association is comprised of a single lithofacies, an algal laminite. This facies is characterized by crinkled laminated lime mudstone forming thick cm– to dm–scale mats, which commonly exhibit mud cracks (Fig. 6A). In thin section, the facies appears to be composed entirely of lime mud with some peloids, with no readily discernible skeletal framework. Allochthonous grains, including rip-up mud clasts and rounded *Lithocodium/Bacinella*-coated clasts, may be entrained in the mats or form thin beds between mats. The laminated, matted fabric, rip-up clasts, and mud cracks suggest that this facies was deposited in a tidal flat setting.

Facies Association 2: High-Energy Shallow Subtidal

Four lithofacies are assigned to the high-energy shallow subtidal facies association, characterized by well-washed (i.e., mud-free) grainstones and mud-poor grain-dominated packstones, composed of abundant allochems associated with shallow subtidal deposition. The ooid grainstone to grain-dominated packstone consists of well-developed radial ooids, many of which are partially micritized (Fig. 6B). Discernible ooid nuclei include molluscan fragments, echinoid fragments, and peloids. Narrow rims of isopachous equant calcite cement surround most ooids; the original pore space between allochems is largely filled

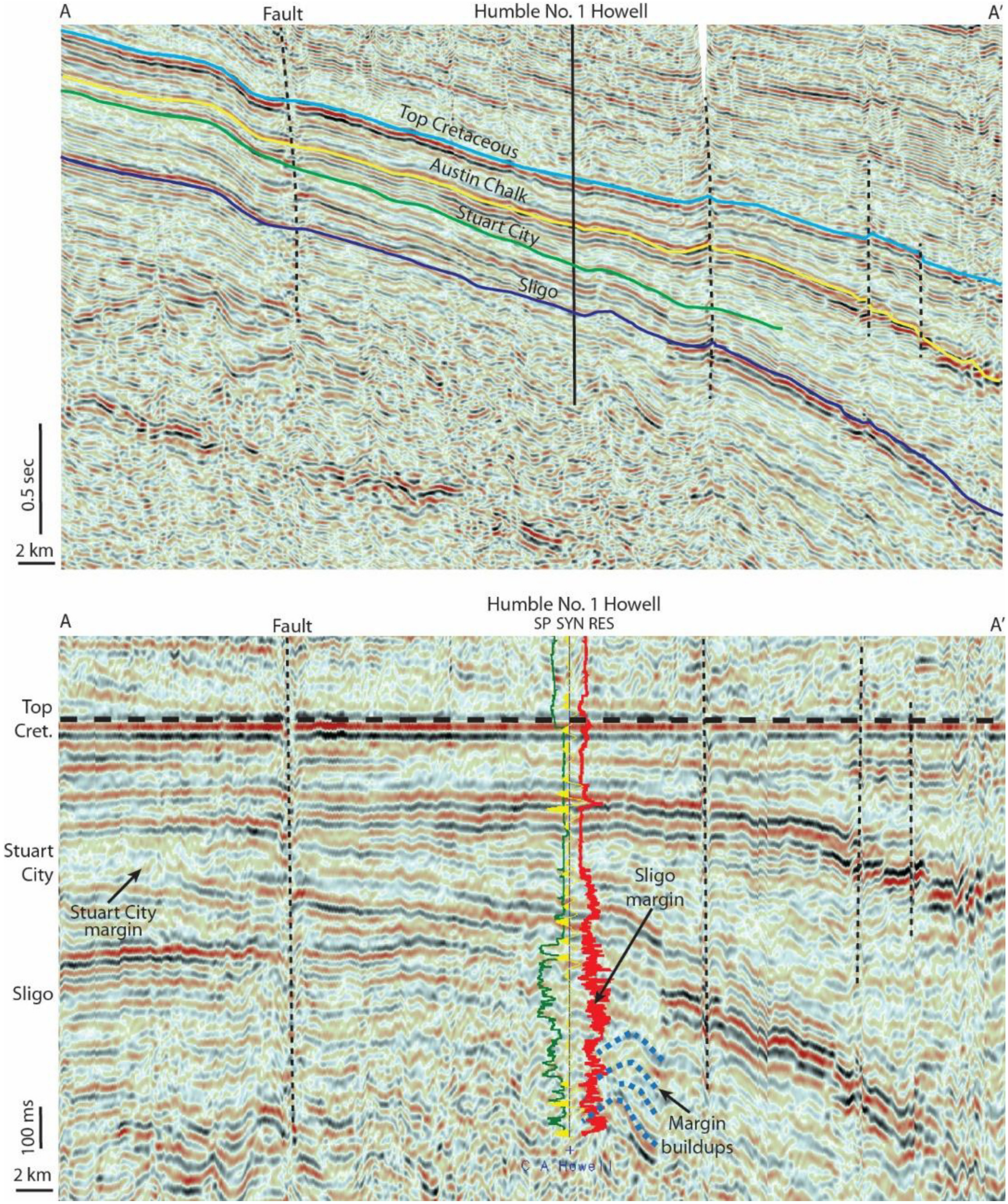

Figure 4. GulfSpan GSM3–2150 2D seismic line showing the location of the core relative to Sligo and Stuart City (Edwards) shelf margins. The top panel (unflattened) shows the architecture of the present-day Cretaceous platform; the bottom panel shows the same interval, flattened on top of the Cretaceous. Major formation boundaries are labeled, and annotations show faults and seismic facies (buildups) of note. Seismic authorized for publication courtesy of Fairfield Geotechnologies.

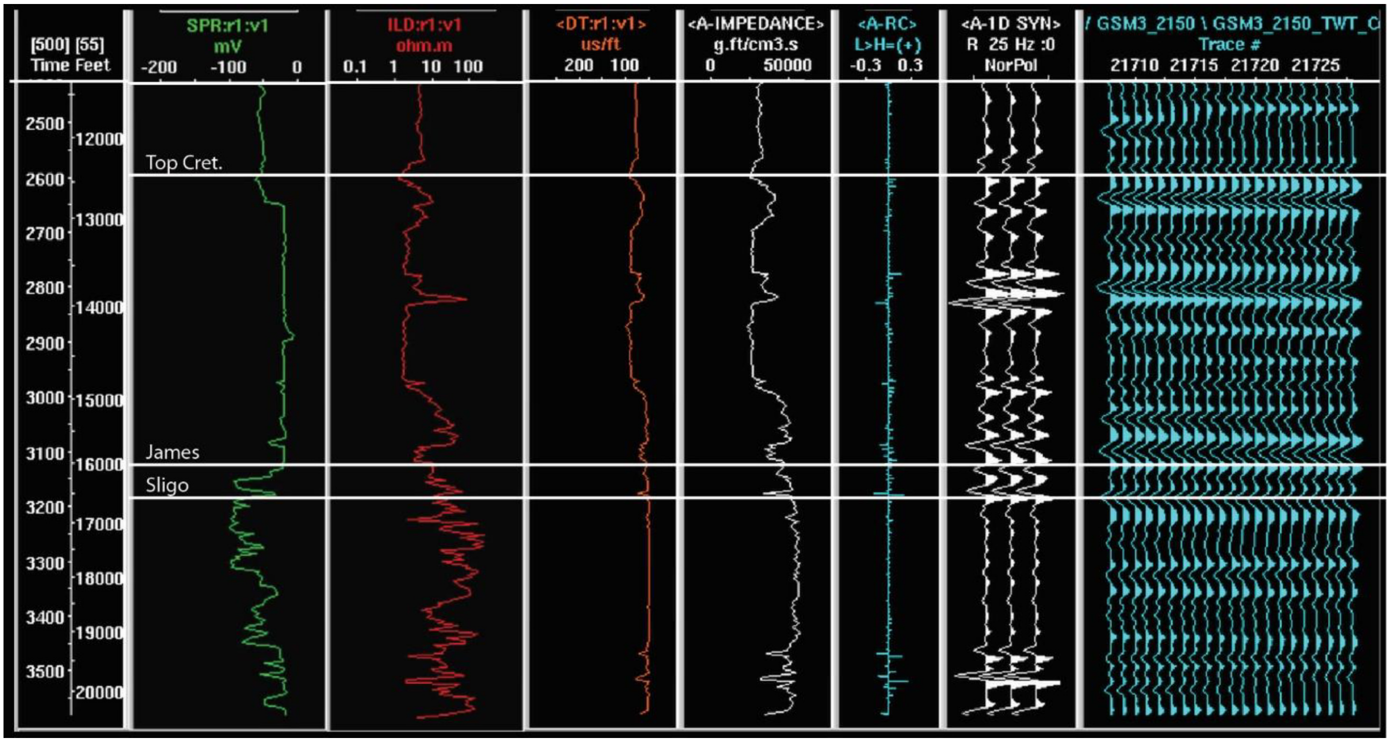

Figure 5. Synthetic seismogram for the Humble No. 1 Howell well projected to seismic line A–A'. The impedance log is calculated from the acoustic (delta time) log and Gardner's equation.

by blocky equant calcite cement, although some mud drapes and peloids are observed filtering down between ooids. The well-developed ooids and paucity of uncoated skeletal allochems or lime mud suggest deposition in a high-energy shoaling environment.

An ooid-gastropod packstone-rudstone, which consists dominantly of a mix of ooids and large intact high-spired gastropods in a lime mud matrix (Fig. 6C), is found in close association with the ooid grainstones to grain-dominated packstones (Fig. 7). Gastropod shells were originally aragonitic, and have been dissolved and subsequently replaced by coarse crystalline equant calcite. Other subordinate allochems include reworked fragments of red algae, oysters, formerly aragonitic bivalves, green algae, and echinoids. Whereas the ooid grainstone is interpreted to represent the main shoal body (i.e., ooid factory), the ooid-gastropod packstone-rudstone is suggestive of a lower-energy setting adjacent to the main shoal, such as a tidal channel or the margin of the shoal complex bordering a lower-energy lagoon facies.

Coarse skeletal grainstones-rudstones occur throughout the core, with variable skeletal compositions depending on the juxtaposition of facies. In general, they are composed of coarse-grained, poorly-reworked, and poorly-sorted skeletal fragments and intraclasts (Fig. 6D). Oyster and rudist fragments are the dominant grain type, with coral, red algae, benthic foraminifers, and echinoid fragments occurring in minor amounts. Abundant micritic intraclasts may be reworked rip-up clasts, but may also include similar-appearing reworked fragments of *Lithocodium/Bacinella* encrustations that can only be identified when the relict skeletal structure is preserved. The coarse-grained, poorly-sorted texture and the abundance of reef-associated fauna suggest deposition in a periodically high-energy back-reef environment, where grains were sourced from the reef flat by waves, currents, and storms.

Fine miliolid-peloid grainstones are common at the top of the core, occurring in planar-bedded to massive packages up to 10 ft thick (Fig. 7). Chiefly composed of well-sorted miliolids and peloids, this facies may locally include fine echinoid and oyster fragments, other benthic foraminifers, and rare larger cm-scale fragments of toucasid rudists (Fig. 6E). Some "peloids" may be small fragments of *Lithocodium/Bacinella*. Still, relict skeletal structures are difficult to identify at the small scale of these allochems. The degree of sorting, allochem types, and rock

(FACING PAGE) Figure 6. Facies of the cored Sligo intervals in the No. 1 Howell well. (A) Algal laminite deposited in a tidal flat setting. Prominent mudcracks are visible. Several layers of intraclasts are also present. 18,155 ft. (B) Ooid grainstone. Note draped peloids across some grains and that pore space is occluded by equant cement. 18,044 ft. (C) Ooid-gastropod rudstone/packstone. Large high-spired gastropods dominate. 18,034 ft. (D) Coarse skeletal rudstone. Note poor sorting and variable degree of reworking and hydrodynamic orientation of larger molluscan fragments. 17,938 ft. (E) Fine miliolid-peloid grainstone. Note sorting and size of allochems compared to that shown in D. 17,853 ft. (F) Skeletal-miliolid-green algae-peloid wackestone/packstone. Black arrows point to miliolids. White arrows indicate large fragments of calcareous green algae. 18,004 ft. (G) Caprinid rudstone/floatstone. Caprinids are largely intact and upright. The black arrow points to borings. 18,151 ft. (H) Toucasid rudstone/floatstone. Toucasids grow in close association with one another (possibly attached) in a muddy matrix. 17,872 ft. (I) Oncolitic *Lithocodium/Bacinella*-encrusted skeletal rudstone. Note the large, ragged, laminated texture of the oncoids, possibly Lithocodium/Bacinella coatings. 18,188 ft. (J) Argillaceous skeletal-oncoid wackestone/packstone with interbedded microbial packstone. The white arrow points to a microbially-coated grain, whereas the black arrows point towards microbial binding between many grains. 17,974 ft. (K) Argillaceous mudstone; note that clays are concentrated in wispy dissolution seams. 18,057 ft.

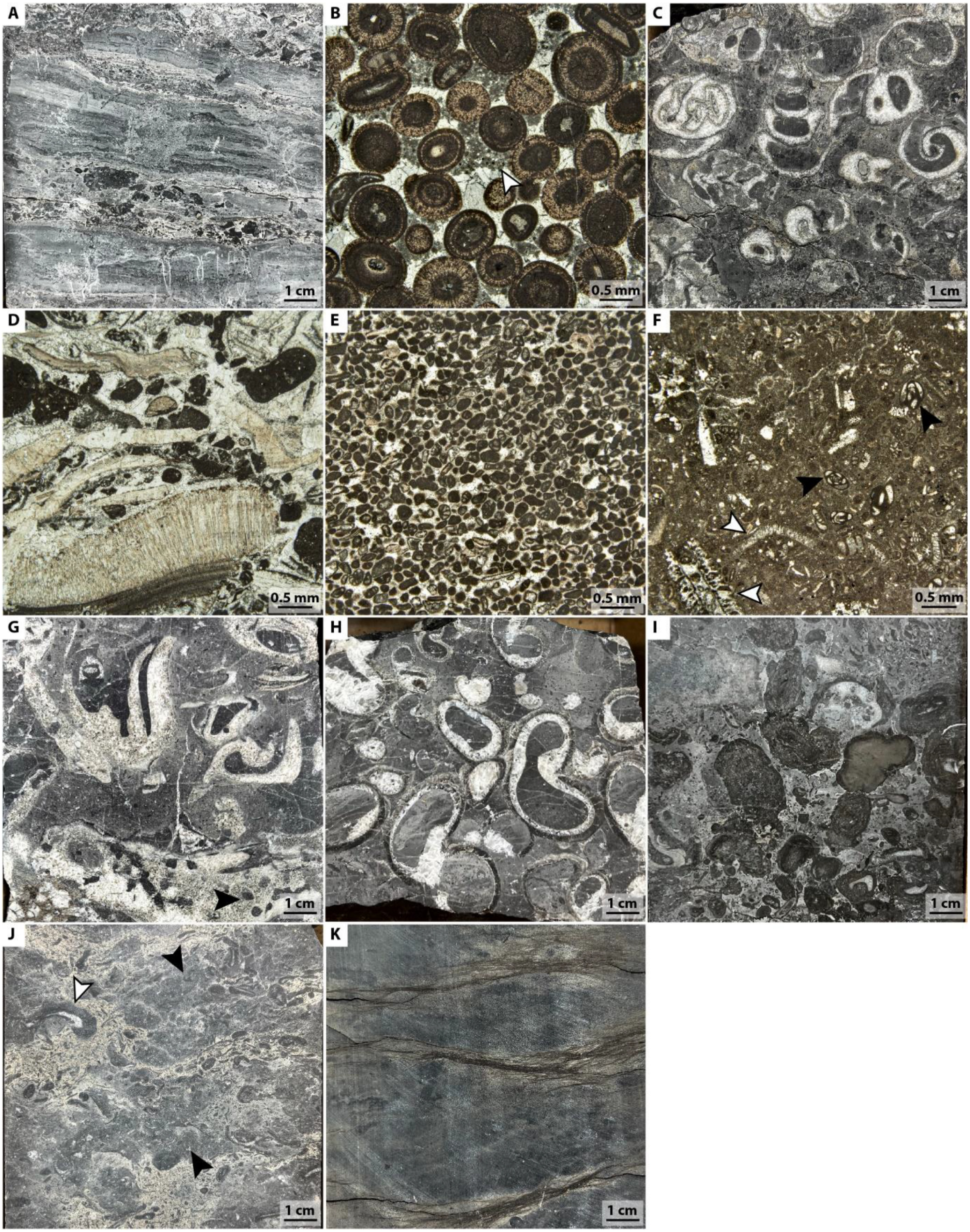
A
1 cm
B
0.5 mm
C
1 cm
D
0.5 mm
E
0.5 mm
F
0.5 mm
G
1 cm
H
1 cm
I
1 cm
J
1 cm
K
1 cm

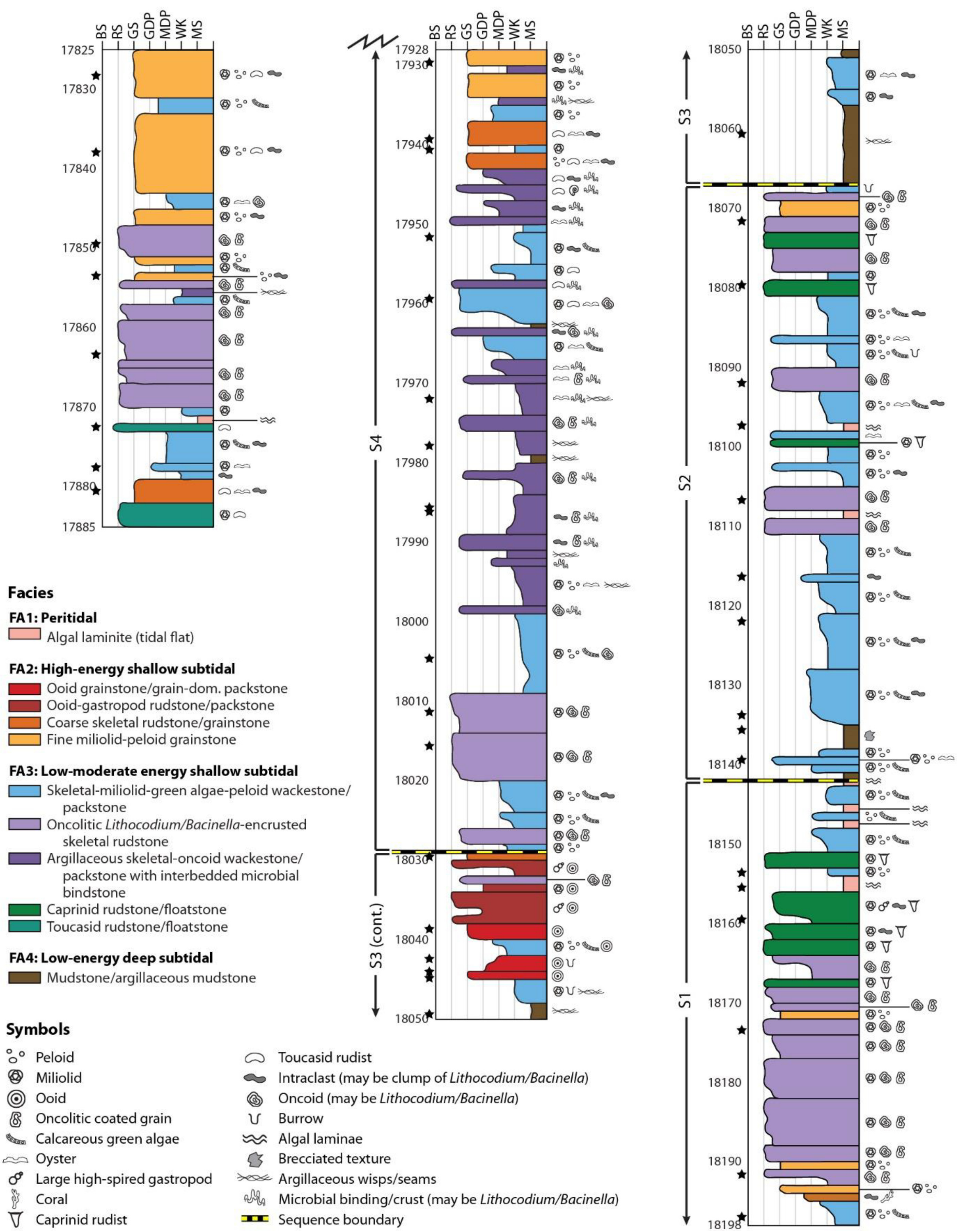

Figure 7. Core description of the Sligo interval in the No. 1 Howell well. Sequences 1 through 4 are labeled (S1–S4). Stars indicate the locations of thin sections.

fabric all suggest deposition in a shallow-water environment, perhaps where shelf sediments were winnowed by current activity.

Facies Association 3: Low- to Moderate-Energy Shallow Subtidal

FA3 consists of five lithofacies, each of which is generally mud-dominated but otherwise differentiated by mineralogy, dominant allochems, and abundance and character of microbial elements/constituents. Skeletal-miliolid-green algae-peloid wackestones/packstones occur commonly throughout the core and are characterized by a diverse variety of allochems in a lime mud matrix (Fig. 6F). Locally, it may occur as a rudstone depending on the occurrence of larger fossils such as toucasid rudists and oysters. Allochem constituents, in order from greatest to least abundance, include peloids, calcareous green algae, miliolids, oysters, echinoids, toucasid rudists, other molluscan fauna, other benthic foraminifers, gastropods, and small oncoids which may be *Lithocodium/Bacinella*-encrusted grains. Benthic foraminifers identified from samples of this facies include *Paracoskinolina sunnilandensis* and *Choffatella decipiens*. Allochems are poorly sorted, and very few are significantly abraded, suggesting minor transport distance before final deposition. The diverse fauna is characteristic of a low-energy, shallow-water environment, likely a distal back-reef/back-reef lagoon setting associated with a shelf-margin complex. *C. decipiens* has previously been linked to back-reef and back-reef lagoon environments, supporting this interpretation (Selvius and Wilson, 1985).

Caprinid rudstones/floatstones are common in the lower portion of the core, occurring only below the thick mudstone encountered in the 18,057–18,067 ft interval. Large, intact caprinids and subordinate caprinid fragments are surrounded by miliolids and other benthic foraminifers, skeletal fragments, and peloids, in a matrix with varying amounts of lime mud (Fig. 6G). Fragments of coral, stromatoporoids, red algae, gastropods, recrystallized mollusks, and echinoids are present. Although many caprinids have been toppled, partially fragmented, abraded, and bored, some appear to remain intact and upright in life position, suggesting that little to no transport occurred. Past work has identified that caprinid-dominated communities are common in a variety of environments ranging from shelf-margin shoal complexes to reef proper to back-reef (e.g., Bebout et al., 1981; Kirkland et al., 1987; Collins, 1988; Scott, 1988, 1990; Wilson and Ward, 1993; Skelton and Gili, 2012); some studies recognized differences in the depositional environment based on caprinid morphology (upright "elevator" vs. recumbent; e.g., Collins, 1988; Scott, 1990; Ross and Skelton, 1993; Hofling and Scott, 2002). Here, we suggest a moderate-energy semi-protected back-reef setting based on the presence (but not abundance) of reef-derived detritus, indicating proximity to the reef, and lesser energy setting indicated by the upright character of the caprinids as well as the presence of a large proportion of lime mud and miliolids.

Toucasid rudstone/floatstones are uncommon in the cored interval and only occur in the uppermost portion (Fig. 7). Clumps of toucasids, some appearing to be attached, rest in a lime mud matrix (Fig. 6H). Subordinate allochems include miliolids, other benthic foraminifers, peloids, calcareous green algae, and a variety of echinoid and molluscan fragments, suggesting a shallow, low-energy depositional setting, likely a distal back-reef to lagoon environment within a shelf-margin complex.

Oncolitic *Lithocodium/Bacinella*-encrusted skeletal rudstones are common throughout the cored section, occurring as thick packages most commonly in association with the skeletal-miliolid-green algae-peloid wackestone/packstone facies. Thick laminated microbial coatings encrusting cm-scale skeletal fragments form large, irregularly-shaped oncoids up to 3 in wide (Fig. 6I). Petrographic analysis of the microbial coatings reveals that they may exhibit distinguishable *Lithocodium/Bacinella* skeletal structures, but mostly have non-diagnostic laminated micritic textures. Therefore, we refer to these allochems generally as oncoids, although some may more accurately be *Lithocodium/Bacinella*-coated grains. The nuclei of these grains consist of molluscan, echinoid, rudist, and coral fragments. Other associated allochems include abundant miliolids, benthic foraminifers, and calcareous green algae; echinoids and formerly aragonitic molluscan fragments are common. Lime mud fills spaces between grains. The large, irregular texture of the oncoids and the abundance of mud and shallow-water fauna indicate a shallow subtidal depositional setting in a low- to moderate-energy regime, most likely in a protected distal back-reef/lagoon. Oncoids may have been sporadically rolled around on the seafloor by episodic increases in currents or storm-related events, causing the ragged texture with irregular growth.

In the middle interval of the core, the oncolitic *Lithocodium/Bacinella*-encrusted skeletal rudstone transitions into an argillaceous skeletal-microbial bindstone interbedded with skeletal-oncoid wackestone/packstone (Fig. 7). The skeletal-oncoid wackestone/packstone component is similar in allochem composition to the oncolitic *Lithocodium/Bacinella*-encrusted skeletal rudstone, but the oncoids are much smaller, with diameters less than 2 cm. It occurs as thin beds gradationally interbedded between thicker intervals of microbially bound skeletal wackestone-bindstone. The skeletal-microbial bindstone is characterized by abundant benthic foraminifers (including miliolids, *P. sunnilandensis* and *C. decipiens*, and other unidentified foraminifers) as well as calcareous green algae (mostly dasycladacean) and occasional oncoids, bound together by a clotted microbial fabric that is readily visible in core (Fig. 6J). Although the macrofabric appears somewhat thrombolitic (sensu original definition in Aitken [1967]), thin-section analysis reveals mostly featureless dense micrite, with no relict structures (e.g., mesoclots, laminae, or dendritic features) that indicate a more organized microbial origin. Therefore, here we only designate this facies as being generally microbial and suggest that the origin of the clotted fabric could have been calcified bacterial components, such as proposed by Riding (2000). Entrained fossil allochems are commonly nearly intact, including large stems of dasycladacean green algae, suggesting a low-energy setting with minimum transport and reworking. We interpret a somewhat deep-water protected lagoon setting based on the foraminifer-dominated fauna, abundance of undisturbed microbial binding, and lack of reworking of allochems.

Facies Association 4: Low-Energy Deep Subtidal

An argillaceous carbonate mudstone represents the low-energy deep subtidal regime. Dark gray with clay concentrated in argillaceous seams, it is nearly devoid of fossils aside from the occasional highly-abraded molluscan or echinoid fragments (Fig. 6K). Where it is juxtaposed above facies associated with shallow subtidal or peritidal environments, it may be dolomitized or may contain brecciated rip-up clasts. Thus, it is interpreted to represent a deeper water (but likely not below storm-weather wave base) subtidal setting probably associated with transgression during pulses of sea-level rise.

Stacking Patterns and Overall Trends

Seismic facies indicative of large-scale reef buildups can be readily identified in seismic dip sections (Bubb and Hatlelid, 1977; Zampetti et al., 2004). In seismic section A–A', mound and back-mound seismic facies are observable in the Sligo interval (Fig. 4). When projected onto the seismic line, the No. 1 Howell well plots in the back-mound (back-reef and back-reef lagoon portion of the shelf-margin complex) setting, providing supporting evidence for the back-reef depositional environment interpreted for the majority of the facies observed in the investigated core.

The interval of Sligo Formation recovered in the No. 1 Howell core is dominantly composed of muddier (i.e., lime mud) facies with abundant microbial and algal material, *Lithocodium/Bacinella* encrustations, benthic foraminifers, and molluscan fauna. Although the majority of the lithofacies differentiated here are generally associated with a back-reef setting within a shelf-margin complex, facies stacking patterns suggest minor shifts in depositional environment over time, which can be linked to eustatic sea-level trends and subordinate changes in energy regime. Although facies are largely muddy and oncolitic throughout the core and biota remain the same, skeletal debris grainstones increase in thickness and abundance up-section. This may reflect greater wave energy acting upon the shelf margin, or increased storm activity. Four sequences were identified in the core based on these trends: sequence 1, spanning 18,142–18,198 ft depth (base of core 1); sequence 2, spanning 18,067–18,142 ft depth; sequence 3, spanning 18,029–18,067 ft depth; and sequence 4, beginning at 18,029 ft depth and extending up to the top of core 1 at 17,098 ft (Fig. 7). Because of a break in core with a 43 ft gap, the upper portion of the cored Sligo interval (core 2; 17,825–17,885 ft) is not assigned to a sequence as its relationship with the underlying sequence (sequence 4, 17,928–18,028 ft, in core 1) is unclear.

Sequence 1 is dominated by oncolitic *Lithocodium/Bacinella*-encrusted skeletal rudstones, which grade upsection into caprinid rudstone/floatstone, which persists for approximately 15 ft. Above that, the section transitions into interbedded intervals of skeletal-miliolid-green algae-peloid wackestone/packstone and algal laminite. This shallowing-upwards sequence is thus observed to transition from a lower-energy subtidal back-reef setting into a higher-energy more proximal back-reef setting and finally into a peritidal setting, suggesting aggradation of the shelf-margin complex up to or near sea level.

Sequence 2 is dominated by lower-energy, muddier subtidal facies, mainly skeletal-miliolid-green algae-peloid wackestone/packstones. At the base of the section, initial transgression is represented by a dolomitized argillaceous lime mudstone, which grades upwards into low-energy shallow-water facies. Some very thin algal laminites are observed in the center of the section between various other facies association 3 facies. The uppermost portion of the sequence grades into caprinid rudstone/floatstones with heavily abraded caprinids; the sequence cap is a peloidal grainstone with mud rip-up clasts and large bivalve fragments. The overall low-energy, very shallow subtidal to peritidal facies in sequence 2 suggest deposition in a protected, low-energy setting at or near sea level, perhaps behind an emergent portion of the margin complex. Rip-up clasts and large bivalve fragments may be attributed to the periodic influence of storms.

Sequence 3 is characterized by a thick interval of argillaceous carbonate mudstone, followed by a fairly short transition up-section from skeletal-miliolid-green algae-peloid packstone into ooid grainstones and ooid-gastropod rudstones. This stacking pattern likely reflects partial drowning across even the topographically highest parts of the shelf-margin complex during rapid transgression, followed by the establishment of a high-energy oolitic shoal on the topographic high during regression.

Sequence 4 is incompletely preserved because of a break in the core at 17,928 ft. At its base, low-energy muddy skeletal-miliolid-green algae-peloid wackestones/packstones alternate with intervals of oncolitic *Lithocodium/Bacinella*-encrusted skeletal rudstone in a stacking pattern similar to that observed in sequence 2. At a depth of approximately 18,000 ft, these facies are followed by a thick interval of argillaceous skeletal-oncoid wackestone with interbedded microbial bindstone, indicating deepening and transition into a more protected, lower-energy lagoon setting. Upsection, these facies pass into fine miliolid-peloid grainstones and coarse skeletal grainstones, suggesting shallowing and accompanying increase in wave energy. The magnitude of sea-level fall is unknown here because incomplete coring eliminates the ability to identify a sequence boundary conclusively.

Although core 2 does not record a complete definable sequence, it does exhibit a shallowing-upward character, with muddier low-energy subtidal facies (toucasid rudstone/floatstone, skeletal-miliolid-green algae-peloid wackestone/packstone, oncolitic *Lithocodium/Bacinella*-encrusted skeletal rudstone) transitioning up-section into thick packages of fine miliolid-peloid grainstone. The fine miliolid-peloid grainstone commonly includes larger toucasid and oyster fragments, indicating that toucasids likely lived nearby. In general, all facies within this cored interval can be attributed to a distal back-reef to lagoon environment, but the upper grainstones suggest an increase in wave energy that winnowed shelf sediments, likely related to reduced accommodation.

It is important to note that the stacking patterns are recognizable at two scales: at a sequence scale of tens of ft (facies associations) and at a smaller ft-scale (individual facies). The stacking patterns are considered to reflect long-term deposition of a stable back-reef setting on a passive margin platform during variations in eustatic sea-level or changes in local environmental conditions (e.g., storm intensity or variations in circulation related to changing reef or margin complex morphology). The documentation of these facies changes aids in understanding depositional heterogeneity over long periods.

PARAGENETIC EVOLUTION OF PORE NETWORK

Multiple generations of diagenesis ranging from early marine to late burial processes are identified in the No. 1 Howell core (Fig. 8). The paragenetic sequence outlines observed diagenetic features relative to the general diagenetic environment (marine, meteoric, shallow subsurface, and deep subsurface) in which the features formed. Biota exhibit a mixed mineralogy of calcite (e.g., oysters), Mg–calcite (e.g., echinoids, benthic foraminifers, *Lithocodium/Bacinella*), and aragonite (bivalves, gastropods, green algae, rudists, corals); each mineralogy reacts differently to varying diagenetic processes (Land, 1967).

In the marine environment (Fig. 8), allochems are relatively stable and resistant to chemical diagenesis but are susceptible to mechanical and biological diagenesis. Many skeletal grains are prone to fragmentation by physical (e.g., wave and current action) and biological (bioturbation and boring) processes. Fragmentation reduces grain size, thus reducing interparticle pore size and also destroys intraparticle pores by shell breakage. The marine environment is also associated with the formation of micrite envelopes around many grains; the envelopes are Mg–calcite and are stable during later dissolution of the aragonitic skeletal fragments (Winland, 1968). *Lithocodium/Bacinella* encrustations also coat grains. These encrustations are Mg–calcite and stable relative to macrodiagenetic dissolution (Loucks et al., 2013) and preserve the outlines of former aragonitic skeletal fragments that have undergone dissolution.

Calcite grains in the meteoric environment are stable, but aragonite and Mg–calcite grains undergo diagenesis (Land, 1967). Aragonite grains generally dissolve and are refilled partly or entirely by fine to medium crystalline, equant calcite and, more rarely, by coarse crystalline, equant calcite. Mg–calcite in the studied core stabilized to low Mg–calcite by recrystallizing at the microscale to fine crystalline, microrhombic calcite, as demonstrated by Loucks et al. (2013). This diagenetic process produces micropores, which become the main pore network at deep burial depths.

In the shallower subsurface diagenetic environment (within a few hundreds of feet of burial), Mg–calcite grains are interpreted to become fully stabilized to low Mg–calcite (Loucks et al.,

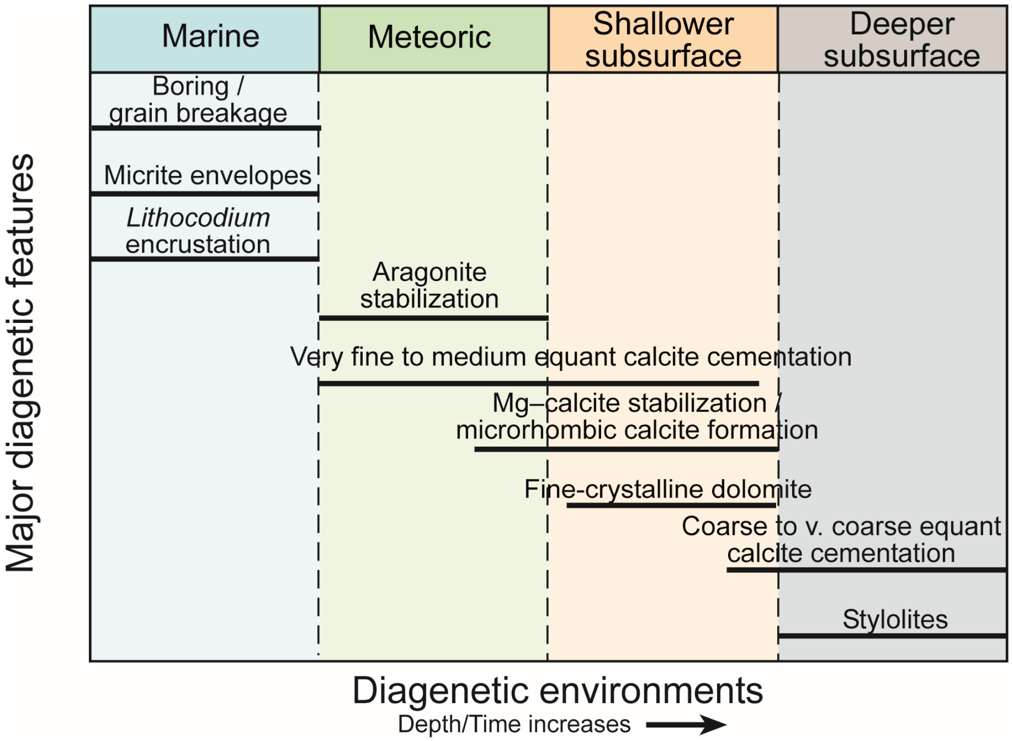

Figure 8. Paragenesis of diagenetic features observed in the No. 1 Howell core.

2013). Very fine to medium crystalline, equant calcite continued to be precipitated, probably along with rarer coarse crystalline calcite in interparticle and moldic pores. Some fine crystalline dolomite was precipitated.

The late diagenetic environment in the deeper subsurface is associated with coarse to very coarse crystalline, equant calcite cement precipitation that further occludes macropores. Stylolites generated in this stage reduced rock volume and simultaneously functioned as a source of calcium carbonate for burial cementation. In the No. 1 Howell core, this diagenesis stage was responsible for destroying the macropore network. Micropores remained unaffected by burial cementation.

PORE SYSTEMS AND RESERVOIR QUALITY

Few existing studies characterize the pore network in the Sligo margin (e.g., Bebout et al., (1981), and Loucks, (2019)). Thus the pore network documented in the No. 1 Howell core provides valuable additional data to expand our understanding of this system. Bebout et al. (1981) documented a suite of pore types in different Sligo facies associated with the back-reef and shelf margin bank complexes in South Texas, including intraparticle, interparticle, moldic, and micropores. In some facies (e.g. their pellet grainstone, oncolite packstone, coated-grain packstone, pellet packstone, and skeletal grainstone), some moldic porosity and a modest amount (<5%) of interparticle porosity were documented. Up to 10% estimated interparticle and intraparticle porosity was observed in the skeletal and oolite grainstone facies in one core. Other facies (e.g., laminated lime mudstone, oyster-miliolid wackestone, toucasid wackestone, oncolite packstone, fossiliferous lime mudstone) had no observed porosity or local development of micropores.

In contrast, in the Sligo margin in East Texas, primary porosity has been completely destroyed by compaction and occlusion by late-stage, equant calcite cements. The remaining pore network is composed of micropores in all facies (Fig. 9). As micropore networks in Cretaceous reef margins are particularly understudied, documenting the distribution and development of micropore networks here is crucial to improving our understanding. Perkins (1989), Loucks et al. (2013), and Loucks (2019) addressed the origin and characteristics of microrhombic calcite development and associated micropores in the Sligo and Stuart City shelf-margin complexes along the onshore Texas Gulf Coast. Loucks et al. (2013) and Loucks (2019) observed that all macropores have been occluded at 15,000 ft or greater depths, allowing the micropores that formed at shallower burial depths to become the major pore network.

Reports vary on the control of lithofacies and grain type on porosity and permeability in Texas Cretaceous shelf margins. Waite (2009) reported significant variation in reservoir properties across several fields in a 250 mi span of Stuart City and Sligo reef margin in South Texas. In most fields, lithofacies were a primary control on porosity and permeability; however, the most productive facies were shown to vary (e.g., bioherms and reef-derived grainstones in Washburn Ranch Field and microporous mudstones in Word Field). Loucks et al. (2013) found a positive correlation between micropore-related porosity and grain type in the Stuart City Pawnee Field of South Texas proposed that the primary mechanism of micropore development was the conversion of Mg–calcite allochems to low Mg–calcite by dissolution and reprecipitation.

Conversely, although they did note the potential for better micropore development in some Mg–calcite grains (e.g., miliolids and red algae), Van Simaeys et al. (2017) found no facies or grain type control in their study of porosity and permeability of the Edwards (Stuart City) Word Field, showing instead that the micropore network was well-established in both grainstones and muddier facies through grain-to-grain contacts and micritic matrix, respectively. Loucks (2019) did emphasize the importance of micropores network supporting deep gas production. In the absence of a facies control, reservoir quality is instead related to position on a structural high, which Van Simaeys et al. (2017) attribute to limitation of later diagenetic calcite precipitation due to hydrocarbons filling the available pores.

The pore network documented in the No. 1 Howell core further highlights the high potential for pore development/

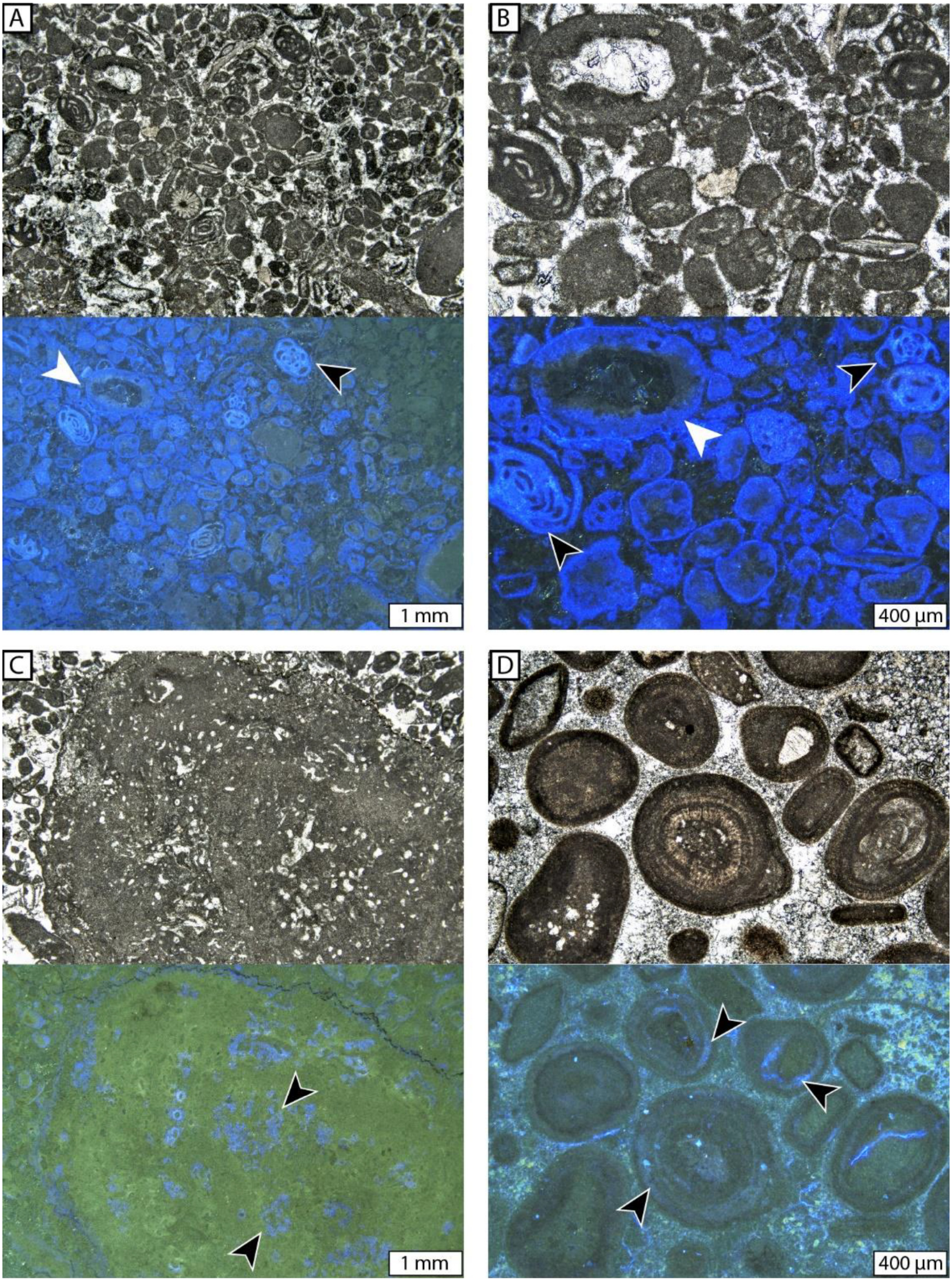
A
1 mm
B
400 µm
C
1 mm
D
400 µm

(FACING PAGE) Figure 9. Microporosity in thin sections highlighted by blue fluorescent dye. (A) Fine miliolid-peloid grainstone demonstrating enhanced micropores in originally Mg–calcite grains (miliolids, black arrow; *Lithocodium/Bacinella* coating, white arrow) and rims of peloids. 17,828 ft. (B) Close-up of A. (C) Thick *Lithocodium/Bacinella* coating on a skeletal grain (not pictured) demonstrating variability in micropores within the coating. Black arrows point to areas of enhanced micropores. 17,828 ft. (D) Microporous layers within ooids (black arrows) in an ooid grainstone.18,042 ft.

preservation variability in these shelf-margin systems. Similar to that observed by Loucks et al. (2013), the micropore network appears to be largely grain-dependent, with the greatest micropore development observed in miliolids, *Lithocodium/Bacinella* coated grains, micrite envelopes, and peloids (Fig. 9). Very few micropores are observed in the micritic matrix, a departure from other reports on micropore networks in Cretaceous reef margins in Texas which describe micropores in micrite as a major contributor to porosity (Loucks et al., 2013; Van Simaeys et al., 2017). Samples from the core exhibit substantially fewer micropores overall, which may be related to burial history. Loucks et al. (2013) and Loucks (2019) documented that micropores develop early in the diagenetic history of carbonates; as deep burial occurs, the macropores cement up while the micropores survive, thus becoming the dominant pore network. However, in ultradeep reservoirs, even the remaining micropores may be destroyed by diagenetic processes (e.g., increased temperature), which may explain the paucity of micropores in micritic sediments in the No. 1 Howell.

Micropores occur more commonly in certain allochems than others (Fig. 9). Miliolids commonly display well-developed micropores (Fig. 9A). Micritic intraclasts, which may be reworked clumps of *Lithocodium/Bacinella*, also contain micropores, with a halo of greater amounts of micropores in the micrite envelopes around their rims (Fig. 9B). Where these grains are densely packed, there is potential for the development of a well-connected pore network. Larger *Lithocodium/Bacinella* encrustations may contain micropores, but it appears that the thicker the encrustation, the fewer micropores are present (Fig. 9C). Some ooids contain micropores, but are not likely to form a connected pore network because the grains are separated by impermeable nonporous calcite cement (Fig. 9D). Loucks et al. (2013) did an in-depth study of micropores in the Stuart City Trend and the reader is referred to that investigation for a detailed discussion of origin of these pores.

DISCUSSION

Depositional Environments

The cored Sligo intervals in the No. 1 Howell well demonstrate some variability, but overall largely represent a back-reef to back-reef lagoon environment. Facies variability can be linked to fluctuations in relative sea level and changes in energy regime, producing stacking patterns that lack well-defined higher-order cyclicity but that can be broadly organized into depositional sequences, which will affect reservoir heterogeneity (Fig. 7). Transgressive deeper subtidal argillaceous mudstones grade upsection into skeletal-miliolid-green algae-peloid wackestones and packstones and oncolitic *Lithocodium/Bacinella*-encrusted skeletal rudstones, facies which are both attributed to shallower water, but still low-energy, settings. Biostromes (caprinid or toucasid floatstones) may occur within these environments. Continued shallowing produces another facies transition into shallow-water, high-energy grainstones, including fine miliolid-peloid grainstones and ooid grainstones; alternatively, facies may grade upwards into algal laminite tidal flats. These intervals represent periods of the lowest relative sea level within each sequence.

No true shelf-margin reef proper facies were cored, but some facies (e.g., coarse skeletal rudstone/grainstone, caprinid rudstone/floatstone) include substantial amounts of reef-derived material that allowed us to make general inferences about the margin character. Various coral and rudist types and some minor stromatoporoid components were observed, suggesting a diverse reef biota with many reef inhabitants filling various niches. Other investigations of cores specifically intersecting the Sligo margin from South Texas (e.g., Bebout, 1977; Bebout et al., 1981; Kirkland et al., 1987; Phelps et al., 2014) reveal similar biotic assemblages, supporting this interpretation and suggesting congruency across this portion of the margin. Seismic facies (Fig. 4) also indicate the presence of a mound (i.e., reef buildup) seaward of the cored well.

Although the shelf margin had significant architectural heterogeneity and variable accretion trajectory across the Gulf of Mexico as a result of differential subsidence and uplift at a local to regional scale (Winker and Buffler, 1988; McFarlan and Menes, 1991; Simo et al., 1993; Goldhammer and Johnson, 2001), studies of various portions of the Sligo margin in Texas overwhelmingly conclude that the margin was initially progradational, then largely aggradational over the remaining duration of growth (Bebout, 1977; Bebout et al., 1981; Kirkland et al., 1987; Winker and Buffler, 1988; Fritz et al., 2000; Phelps et al., 2014). The Fairfield GulfSpan GSM3–2150 seismic line presented here confirms that this holds for the Sligo margin in Tyler County (Fig. 4). This aggradational character can be attributed to a combination of slow, long-term sea-level rise and basin subsidence, and moderate to high carbonate factory productivity, with reef-building organisms able to keep up with sea-level rise, but not outpace it. Commonly, such architectures are associated with the “empty bucket” rimmed shelf model (sensu Schlager [1981, 2003]) in which sedimentation rates at the margin exceed those in the lagoon, creating a localized shallow-water carbonate depocenter at the raised margin rim, with water depth increasing landward from the shelf margin into the back-reef lagoon. Such appears to be the case here, where a significant proportion of the facies documented in core are representative of a low-energy, protected, somewhat deeper subtidal setting landward of the reef margin.

Reef architecture is an overarching control on depositional conditions at the shelf margin, particularly with respect to leeward sedimentation patterns (Immenhauser, 2009). It is important to recognize this contribution, which has the potential to generate facies shifts independent of the commonly-used sea-level-driven model. Where reefs are near enough to sea level to provide an energy barrier, they protect the back-reef, reducing the potential impact of waves and currents and facilitating the deposition of characteristic protected lower-energy facies in the distal back-reef setting (Kench and Brander, 2006; Purkis et al., 2015). Changing morphology of the nearby reef could impact facies deposition and distribution in the back-reef setting by locally modifying energy levels, irrespective of sea-level trajectory. Additionally, major storm events may be responsible for erosion of the reefs, producing event beds of coarse skeletal rudstones and grainstones composed predominately of reef debris (Aigner, 1985; Scoffin, 1993) and that do not appear to be significant sequence caps. Recognizing these relationships is key to limiting over-interpretation in shelf-margin environments, particularly in studies with spatially-restricted data availability, thus the reasonably conservative approach taken here in delineating sequences.

Comparison to South Texas Lower Cretaceous Shelf Margins

Waite (2009) demonstrated that both the Sligo and Stuart City shelf margins have radically different architectures over the span of several counties, dependent on local structural regimes and antecedent topography. He and his collaborators delineated six margin subregions in their area of interest based on different reservoir characteristics, including lithofacies, pore types, burial depth, and architecture; they noted that each subregion required different development strategies because of differences in pore network and reservoir-rock distribution. Thus, characterizing the poorly-known Sligo margin in East Texas is a worthwhile exercise compared to these other, better-known segments of the Sligo and Stuart City margins in South Texas.

As in other areas of Texas, the Sligo margin here is largely aggradational, resulting in only minor deviations in the depositional environment across 373 ft of the core. In general, the facies encountered in the No. 1 Howell well are in good agreement with those documented from comparable intervals of Sligo back-reef in South Texas. Fewer coarse-grained skeletal reef-derived grainstones may indicate that this setting is somewhat more distal from the reef flat and margin than those characterized in South Texas; alternatively, it may indicate lesser erosion related to a quieter energy regime. The higher abundance of mud-dominated facies with large oncoids commonly attributed to quieter, deeper-water back-reef lagoon settings relative to those documented in other Sligo back-reef cores may lend additional support to the former hypothesis over the latter.

Petroleum Potential of Sligo Shelf Margin in East Texas

As in South Texas, the Sligo shelf margin is buried quite deeply in East Texas (17,500–20,000 ft), limiting the potential for economic development because of the dominance of a low-porosity, low-permeability micropore network in potential reservoirs, as well as challenges in drilling deep wells. Despite these challenges, the Sligo has been tested and is a known dry gas producer in fields such as Pawnee and Kenedy SW (Bebout et al., 1981). Here we have shown that a micropore network does exist even in these deeply buried rocks, suggesting that some potential does remain for development. The presence and success of other micropore-dominated shelf margin fields (e.g., Pawnee Field and Word Field) imparts an optimistic outlook for similar possibilities in East Texas, provided that systems with adequate pore connectivity, hydrocarbon migration, and a good top seal can be identified.

East Texas has a complex history, with a large array of structural, architectural, and thermal anomalies that have periodically contributed to uplift and subsidence from the Jurassic through the present (Adams, 2009; Ewing, 2009). Such a complex depositional and burial history is likely to have impacted development of Sligo reservoirs on the margin. Structural highs may present an opportunity for good stratigraphic and structural trapping in a reservoir with greater porosity and permeability. Additionally, less deeply-buried portions of the margin may be less diagenetically affected, with some retention of primary porosity, as documented by Bebout et al. (1981).

CONCLUSIONS

The long cored interval through the Sligo Formation from the Humble No. 1 Howell well provides an opportunity to investigate back-reef depositional settings in a deeply-buried Cretaceous shelf-margin complex and establish a type section for the Sligo back-reef shelf-margin setting in East Texas. As the Sligo margin is poorly known, especially outside of South Texas, this core contributes important insight into formation characteristics, including lithofacies, diagenesis, potential reservoir heterogeneity, and pore network, which will aid in assessing the area for potential development.

Although the core does not cover the complete Sligo interval, it provides evidence of facies types and stacking patterns. Most facies are associated with a back-reef to back-reef lagoon setting but vary based on interpreted energy regime and water depth, which can be attributed to fluctuations in sea level and reef architecture. We identified four depositional sequences, each of which was characterized by a transgressive argillaceous carbonate mudstone at its base, followed by a succession of skeletal-miliolid-green algae-peloid wackestones/packstones, oncolitic *Lithocodium/Bacinella*-encrusted skeletal rudstones, and interbedded microbial bindstones and argillaceous skeletal-oncoid wackestones/packstones representative of a low-energy, shallow-water setting in a distal back-reef to back-reef lagoon environment. Toucasid rudstones or caprinid floatstones, which preserve the remains of biostromes, may also be present in this interval. Peritidal algal laminates or packages of high energy shallow-water ooid or skeletal grainstones cap sequences.

The pore network is composed of micropores, as all original macropores have been occluded by calcite cement. Micropores are generally preferentially present in originally Mg–calcite allochems such as miliolids, peloids, micrite envelopes, and masses of *Lithocodium/Bacinella*. Micritic matrixes are less microporous here than in other documented Sligo margin intervals in South Texas, which may be attributable to the ultradeep burial of the cored interval.

Production success in other Sligo margin fields in South Texas makes the margin an attractive potential gas target in East Texas, depending on economic conditions. However, significant risk is involved related to poorly known reef heterogeneity, deep burial, and associated reduction of potential fluid-flow pathways, etc. Nevertheless, the complex structural and thermal history of East Texas may present some opportunities for productive gas fields if further exploration is conducted.

ACKNOWLEDGMENTS

This study was funded by the State of Texas Advanced Resource Recovery (STARR) Program at the Bureau of Economic Geology, The University of Texas at Austin. The authors would like to thank Fairfield Geotechnologies for their generosity in allowing the use and publication of the GulfSpan 2D seismic line GSM3–2150; it was instrumental in refining ideas and verifying positioning of the core relative to the margin and other features of interest. The authors would also like to thank the staff at the Core Research Center for their assistance in handling and sampling the core. Publication authorized by the Director, Bureau of Economic Geology, Jackson School of Geosciences, The University of Texas at Austin.

REFERENCES CITED

Achauer, C. W., 1977, Contrasts in cementation, dissolution, and porosity development between two Lower Cretaceous reefs in Texas, *in* D. G. Bebout and R. G. Loucks, eds., Cretaceous carbonates of Texas and Mexico: Applications to subsurface exploration: Bureau of Economic Geology Report of Investigations 89, p. 127–137, <https://doi.org/10.23867/RI0089D>.

Adams, R. L., 2009, Basement tectonics and origin of the Sabine Uplift: Gulf Coast Association of Geological Sciences Transactions, v. 59, p. 3–19.

Aigner, T., 1985, Storm depositional systems: Dynamic stratigraphy in modern and ancient shallow-marine sequences: Springer-Verlag, 174 p.

Aitken, J. D., 1967, Classification and environmental significance of cryptalgal limestones and dolomites, with illustrations from the Cambrian and Ordovician of southwestern Alberta: Journal of Sedimentary Petrology, v. 37, p. 1163–1178,

<https://doi.org/10.1306/74D7185C-2B21-11D7-8648000102C1865D>.

Bay, T. A., 1977, Lower Cretaceous stratigraphic models from Texas and Mexico, *in* D. G. Bebout and R. G. Loucks, eds., Cretaceous carbonates of Texas and Mexico: Applications to subsurface exploration: Bureau of Economic Geology Report of Investigations 89, p. 12–30, <https://doi.org/10.23867/RI0089D>.

Bebout, D. G., and R. G. Loucks, 1974, Stuart City Trend, Lower Cretaceous, South Texas: A carbonate shelf-margin model for hydrocarbon exploration: Bureau of Economic Geology Report of Investigations 78, 80 p., <https://doi.org/10.23867/RI0078D>.

Bebout, D. G., 1977, Sligo and Hosston depositional patterns, subsurface of South Texas, *in* D. G. Bebout and R. G. Loucks, eds., Cretaceous carbonates of Texas and Mexico: Applications to subsurface exploration: Bureau of Economic Geology Report of Investigations 89, p. 79–96, <https://doi.org/10.23867/RI0089D>.

Bebout, D. G., R. A. Schatzinger, and R. G. Loucks, 1977, Porosity distribution in the Stuart City Trend, Lower Cretaceous, south Texas, *in* D. G. Bebout and R. G. Loucks, eds., Cretaceous carbonates of Texas and Mexico: Applications to subsurface exploration: Bureau of Economic Geology Report of Investigations 89, p. 97–126, <https://doi.org/10.23867/RI0089D>.

Bebout, D. G., D. A. Budd, and R. A. Schatzinger, 1981, Depositional and diagenetic history of the Sligo and Hosston Formations (Lower Cretaceous) in South Texas: Bureau of Economic Geology Report of Investigations 109, 70 p., <https://doi.org/10.23867/RI0109D>.

Bubb, J. N., and W. G. Hatlelid, 1977, Seismic stratigraphy and global changes of sea level, part 10: Seismic recognition of carbonate buildups, *in* C. E. Payton, ed., Seismic stratigraphy—Applications to hydrocarbon exploration: American Association of Petroleum Geologists Memoir 26, p. 185–204, <https://doi.org/10.1306/m26490c12>.

Cohen, K. M., S. C. Finney, P. L. Gibbard, and J. X. Fan, 2013, The ICS international chronostratigraphic chart: Episodes, v. 36, p. 199–204.

Cohen, K. M., D. A. T. Harper, P. L. Gibbard, and N. Car, 2023, International chronostratigraphic chart: International Commission on Stratigraphy, 1 p., <http://www.stratigraphy.org/ICSchart/ChronostratChart2023-04.pdf>.

Collins, L. S., 1988, The faunal structure of a mid-Cretaceous rudist reef core: *Lethaia*, v. 21, p. 271–280, <https://doi.org/10.1111/j.1502-3931.1988.tb02079.x>.

Cook, T. D., 1979, Exploration history of South Texas Lower Cretaceous carbonate platform.: American Association of Petroleum Geologists Bulletin, v. 63, p. 32–49, <https://doi.org/10.1306/c1ea55b2-16c9-11d7-8645000102c1865d>.

Ewing, T. E., 1991, Structural framework, *in* A. Salvador, ed., The geology of North America, v. J: The Gulf of Mexico Basin: Geological Society of America, p. 31–52, <https://doi.org/10.1130/DNAG-GNA-J.31>.

Ewing, T. E., 2009, The ups and downs of the Sabine Uplift and the northern Gulf of Mexico Basin: Jurassic basement blocks, Cretaceous thermal uplifts, and Cenozoic flexure: Gulf Coast Association of Geological Societies Transactions, v. 59, p. 253–269.

Fritz, D. A., T. W. Belsher, J. M. Medlin, J. L. Stubbs, R. P. Wright, and P. M. Harris, 2000, New exploration concepts for the Edwards and Sligo margins, Cretaceous of onshore Texas: American Association of Petroleum Geologists Bulletin, v. 84, p. 905–922, <https://doi.org/10.1306/e4fd4fc1-1732-11d7-8645000102c1865d>.

Goldhammer, R. Z., and C. A. Johnson, 2001, Middle Jurassic-Upper Cretaceous paleogeographic evolution and sequence-stratigraphic framework of the northwest Gulf of Mexico rim, *in* C. Bartolini, R. T. Buffler, and A. Cantu-Chapa, eds., The western Gulf of Mexico Basin: Tectonics, sedimentary basins, and petroleum systems: American Association of Petroleum Geologists Memoir 75, p. 45–81, <https://doi.org/10.1306/M75768C3>.

Hofling, R., and R. W. Scott, 2002, Early and mid-Cretaceous buildups, *in* W. Kiessling, E. Flügel, and J. Golonca, eds., Phanerozoic reef patterns: Society of Economic Paleontologists and Mineralogists (Society for Sedimentary Geology) Special Publication 72, p. 521–548, <https://doi.org/10.2110/pec.02.72.0521>.

Immenhauser, A., 2009, Estimating palaeo-water depth from the physical rock record: Earth-Science Reviews, v. 96, p. 107–139, <https://doi.org/10.1016/j.earscirev.2009.06.003>.

Jackson, M. P. A., and S. J. Seni, 1983, Geometry and evolution of salt structures in a marginal rift basin of the Gulf of Mexico, East Texas: Geology, v. 11, p. 131–135, <https://doi.org/10.1130/0091-7613(1983)11<131:GAEOSS>2.0.CO;2>.

Kench, P. S., and R. W. Brander, 2006, Wave processes on coral reef flats: Implications for reef geomorphology using Australian case studies: Journal of Coastal Research, v. 22, p. 209–223, <https://doi.org/10.2112/05A-0016.1>.

Kirkland, B. L., R. G. Lighty, R. Rezak, and T. T. Tieh, 1987, Lower Cretaceous barrier reef and outer shelf facies, Sligo Formation, South Texas: Gulf Coast Association of Geological Societies Transactions, v. 37, p. 371–382, <https://doi.org/10.1306/703c7f84-1707-11d7-8645000102c1865d>.

Land, L. S., 1967, Diagenesis of skeletal carbonates: Journal of Sedimentary Petrology, v. 37, p. 914–930, <https://doi.org/10.1306/74d717d5-2b21-11d7-8648000102c1865d>.

Loucks, R. G., F. J. Lucia, and L. E. Waite, 2013, Origin and description of the micropore network within the Lower Cretaceous Stuart City Trend tight-gas limestone in Pawnee Field in South Texas: Gulf Coast Association of Geological Sciences Journal, v. 2, p. 29–41.

Loucks, R. G., C. Kerans, H. Zeng, and P. A. Sullivan, 2017, Documentation and characterization of the Lower Cretaceous (Valanginian) Calvin and Winn carbonate shelves and shelf margins, onshore north central Gulf of Mexico: American Association of Petroleum Geologists Bulletin, v. 101, p. 119–142, <https://doi.org/10.1306/06281615248>.

Loucks, R. G., 2019, Pore networks and reservoir-quality trends in Lower Cretaceous carbonates of the northern rim of the Gulf of Mexico: Substantiating reservoir-quality risk factors: Gulf Coast Association of Geological Sciences Journal, v. 8, p. 35–56.

McFarlan, Jr., E., and L. S. Menes, 1991, Lower Cretaceous, *in* A. Salvador, ed., The geology of North America, v. J: The Gulf of Mexico Basin: Geological Society of America, p. 181–204, <https://doi.org/10.1130/DNAG-GNA-J.181>.

Perkins, R. D., 1989, Origin of micro-rhombic calcite matrix within Cretaceous reservoir rock, West Stuart City trend, Texas: Sedimentary Geology, v. 63, p. 313–321, <https://doi.org/10.1016/0037-0738(89)90138-3>.

Phelps, R. M., C. Kerans, R. G. Loucks, R. O. B. P. Da Gama, J. Jeremiah, and D. Hull, 2014, Oceanographic and eustatic control of carbonate platform evolution and sequence stratigraphy on the Cretaceous (Valanginian-Campanian) passive margin, northern Gulf of Mexico: Sedimentology, v. 61, p. 461–496, <https://doi.org/10.1111/sed.12062>.

Purkis, S. J., G. P. Rowlands, and J. M. Kerr, 2015, Unravelling the influence of water depth and wave energy on the facies diversity of shelf carbonates: Sedimentology, v. 62, p. 541–565, <https://doi.org/10.1111/sed.12110>.

Riding, R., 2000, Microbial carbonates: The geological record of calcified bacterial-algal mats and biofilms: Sedimentology, v. 47, p. 179–214, <https://doi.org/10.1046/j.1365-3091.2000.00003.x>.

Ross, D. J., and P. W. Skelton, 1993, Rudist formations of the Cretaceous: a palaeoecological, sedimentological and stratigraphical review, *in* V. P. Wright, ed., Sedimentology review 1: Blackwell Scientific Publications, p. 73–91.

Schlager, W., 1981, The paradox of drowned reefs and carbonate platforms: Geological Society of America Bulletin, v. 92, p. 197–211, <https://doi.org/10.1130/0016-7606(1981)92<197:TPODRA>2.0.CO;2>.

Schlager, W., 2003, Benthic carbonate factories of the Phanerozoic: International Journal of Earth Sciences, v. 92, p. 445–464, <https://doi.org/10.1007/s00531-003-0327-x>.

Schlager, W., 2010, Carbonate facies models, *in* W. Schlager, ed., Carbonate sedimentology and sequence stratigraphy: Society of Economic Paleontologists and Mineralogists (Society for Sedimentary Geology) Concepts in Sedimentology and Paleontology 8, p. 55–71, <https://doi.org/10.2110/csp.05.08.0055>.

Scoffin, T. P., 1993, The geological effects of hurricanes on coral reefs and the interpretation of storm deposits: Coral Reefs, v. 12, p. 203–221, <https://doi.org/10.2112/05A-0016.1>.

Scott, R. W., 1988, Evolution of Late Jurassic and Early Cretaceous reef biotas: *Palaios*, v. 3, p. 184–193, <https://doi.org/10.2307/3514529>.

Scott, R. W., 1990, Models and stratigraphy of mid-Cretaceous reef communities, Gulf of Mexico: Society of Economic Paleontologists and Mineralogists (Society for Sedimentary Geology) Concepts in Sedimentology and Paleontology 2, 102 p.

Selvius, D. B., and J. E. Wilson, 1985, Lithostratigraphy and algal-foraminiferal biostratigraphy of the Cupido Formation, Lower Cretaceous, Northeast Mexico: Proceedings of the 4th Annual Gulf Coast Section of the Society of Economic Paleontologists and Mineralogists Research Conference, p. 285–311, <https://doi.org/10.5724/gcs.85.04.0285>.

Simo, J. A. T., R. W. Scott, and J. Masse, 1993, Cretaceous carbonate platforms: An overview, *in* J. A. T. Simo, R. W. Scott, and J. P. Masse, eds., Cretaceous carbonate platforms: American Association of Petroleum Geologists Memoir 56, p. 1–14.

Skelton, P. W., and E. Gili, 2012, Rudists and carbonate platforms in the Aptian: a case study on biotic interactions with ocean chemistry and climate: Sedimentology, v. 59, p. 81–117, <https://doi.org/10.1111/j.1365-3091.2011.01292.x>.

Van Simaeys, S., B. Rendall, F. J. Lucia, C. Kerans, and S. Fullmer, 2017, Facies-independent reservoir characterization of the micropore-dominated Word Field (Edwards Formation), Lavaca County, Texas: American Association of Petroleum Geologists Bulletin, v. 101, p. 73–94, <https://doi.org/10.1306/06101616034>.

Waite, L. E., 2009, Edwards (Stuart City) shelf margin of South Texas: New data, new concepts: American Association of Petroleum Geologists Search and Discovery Article 10177, 39 p., <https://www.searchanddiscovery.com/documents/2009/10177waite/>.

Wilson, J. L., and W. C. Ward, 1993, Early Cretaceous carbonate platforms of northeastern and east-central Mexico, *in* J. A. T. Simo, R. W. Scott, and J. P. Masse, eds., Cretaceous carbonate platforms: American Association of Petroleum Geologists Memoir 56, p. 35–49.

Winker, C. D., and R. T. Buffler, 1988, Paleogeographic evolution of early deep-water Gulf of Mexico and margins, Jurassic to middle Cretaceous (Comanchean): American Association of Petroleum Geologists Bulletin, v. 72, p. 318–346, <https://doi.org/10.1306/703C8C22-1707-11D7-8645000102C1865D>.

Winland, H. D., 1968, The role of high Mg calcite in the preservation of micrite envelopes and textural features of aragonite sediments: Journal of Sedimentary Petrology, v. 38, p. 1320–1325, <https://doi.org/10.1306/74d71b6d-2b21-11d7-8648000102c1865d>.

Wooten, J. W., and W. E. Dunaway, 1977, Lower Cretaceous carbonates of central South Texas: A shelf-margin story, *in* D. G. Bebout and R. G. Loucks, eds., Cretaceous carbonates of Texas and Mexico: Applications to subsurface exploration: Bureau of Economic Geology Report of Investigations 89, p. 71–78, <https://doi.org/10.23867/RI0089D>.

Zampetti, V., W. Schlager, J. H. van Konijnenburg, and A. J. Everts, 2004, Architecture and growth history of a Miocene carbonate platform from 3D seismic reflection data; Luconia province, offshore Sarawak, Malaysia: Marine and Petroleum Geology, v. 21, p. 517–534, <https://doi.org/10.1016/j.marpetgeo.2004.01.006>.